Quaternion Estimation for Attitude Determination Using Multiple L1 GPS Receivers

João Cóias[1], José Sanguino[1], Paulo Oliveira[2]

[1]*IT-Instituto de Telecomunicações, Instituto Superior Técnico, Technical University of Lisbon, Lisbon, Portugal*
[2]*ISR-Institute for Systems and Robotics, Instituto Superior Técnico, Technical University of Lisbon, Lisbon, Portugal*
Email: joao.coias@ist.utl.pt; sanguino@lx.it.pt; pjcro@isr.ist.utl.pt

Abstract — **The use of GPS carrier-phase measurements from multiple receivers can be used in the determination of multiple baseline vectors. This can be used for the high precision determination of a vehicle attitude. The use of these measurements requires the determination of the integer carrier phase ambiguities, which is a problem usually addressed with dual-frequency receivers. However, the high cost of these receivers lead to a strong motivation regarding the development of techniques using low-cost single-frequency receivers. In this paper, a high precision attitude determination technique, using a quaternion-based Extended Kalman Filter, based on multiple baselines is proposed, using low cost single frequency L1 GPS receivers. Test results with real data are presented.**

Keywords- Attitude determination, GPS, LAMBDA method, RTK, Ambiguity Filter

I. INTRODUCTION

A vehicle attitude determination can be achieved resorting to multiple GPS receivers and calculating the respective baseline vectors between a reference receiver antenna and the remaining ones. To obtain precise baselines, carrier-phase measurements should be used and, consequently, the unknown integer carrier phase ambiguities must be determined. This problem is usually addressed with expensive dual frequency L1/ L2 GPS receivers, which provide a quick and robust way to determine the unknown integer ambiguities. However, for the low-cost single frequency L1 receivers this is a much harder problem, [1-3]. Thus, in this paper a technique regarding the attitude determination, based on the use of multiple low-cost L1 GPS receivers, is proposed.

From all the techniques that allow the determination of the integer ambiguities, the LAMBDA method is the one that collects most credits, [4-6]. Nevertheless, in a multiple baselines context, the LAMBDA method does not take into account the constraints given by the antennas' disposition. However, some evolutions consider the incorporation the constraints explicitly and hence improve the search process in the LAMBDA method, [7] and [8]. In this paper was decided to use the LAMBDA method along with the Ambiguity Filter, proposed in [9-12], in order to filter the best ambiguity set provided by the LAMBDA method.

For the attitude determination, multiple baselines, fixed with the vehicle body frame, will be used. The technique used to determine the Euler angles is based on the rotation quaternion, which provides a stable and singularity-free estimation.

Finally, the paper is structured as follows. In Section II the system developed for baseline estimation is described. The developed techniques regarding the integer ambiguity resolution are presented in Section III. The quaternion estimation algorithm used for attitude determination is described in Section IV. Section V focus on the test results, which lead to the conclusions presented in Section VI.

II. SYSTEM DEFINITION

A. Introduction

The baseline vector is calculated with RTK techniques. These techniques are based on the use of differences of measurements from two receivers using a common set of satellites. This leads to carrier-phase and code double differences. These double differences are used as observables in the developed system.

B. Single and Double Differences

Carrier-phase and code double differences ($\nabla\Delta$) are used in the baseline vector determination. All the used receivers have to be synchronized. The first step in the computation of the double differences is to generate the single differences (Δ), which correspond to the difference of a satellite measurements provided by two receivers. Thus, for the satellite p and receiver k, one must have the following phase measurements

$$\Phi_k^p = \rho_k^p + \lambda N_k^p + c\left(t_p + t_k + T_k^p + I_k^p\right) + \epsilon_k^p \qquad (1)$$

where

- Φ_k^p is the measured carrier phase (in meters);
- ρ_k^p is the geometric range between the receiver k and the satellite p (in meters);
- λ is the carrier wavelength (in meters);
- N_k^p is the carrier phase integer ambiguity (in cycles);
- c is the speed of light in vacuum (in meters per second);
- t_p and t_k are the satellite and the receiver clock offset (in seconds), respectively;
- T_k^p and I_k^p are the tropospheric and ionospheric delays (in seconds), respectively;
- ϵ_k^p models the disturbance noise due to different factors (hardware, multipath).

Using the carrier phase measurements, to satellite p, from the receiver m, the single differences are given by

$$\begin{aligned}\Delta\Phi_{km}^{p} &= \Phi_{k}^{p} - \Phi_{m}^{p} = \\ &= \Delta\rho_{km}^{p} + \lambda\Delta N_{km}^{p} + c\Delta t_{km} + \Delta\epsilon_{km}^{p}.\end{aligned} \tag{2}$$

In this process the satellite's clock offset is cancelled. Also the tropospheric and ionospheric errors are canceled, assuming that the distance between the receivers is small (less than $50\ km$, accordingly to [2]) when compared with the satellite-receiver distance. However, the clock offset of both receivers are not canceled.

The double differences are obtained with the difference between two single differences. Considering the measurements to satellite q and using equation (2), the double differences are given by

$$\begin{aligned}\nabla\Delta\Phi_{km}^{pq} &= \Delta\Phi_{km}^{p} - \Delta\Phi_{km}^{q} = \\ &= \nabla\Delta\rho_{km}^{pq} + \lambda\nabla\Delta N_{km}^{pq} + \nabla\Delta\epsilon_{km}^{pq}.\end{aligned} \tag{3}$$

This operation eliminates the receiver clock offset.

For code measurements the determination of the double differences is analogous to the one presented in (2) and (3), but without the ambiguity term. So, double differences for code measurements are given by

$$\begin{aligned}\nabla\Delta PR_{km}^{pq} &= \Delta PR_{km}^{p} - \Delta PR_{km}^{q} = \\ &= \nabla\Delta\rho_{km}^{pq} + \nabla\Delta\epsilon_{km}^{pq}.\end{aligned} \tag{4}$$

C. Observation Model

In order to estimate the baseline vector between two antennas, it is necessary to relate it with the double differences. Using interferometric techniques, it is clear that the projection of the baseline onto the line of sight (LoS) between the satellite and the receiver can be represented by the inner product of b with the direction cosine unit vector e^{p}, from the receiver to the satellite. This projection of b is the single difference range between the receivers k and m relative to the satellite p. Thus, single differences of range can be represented as

$$\Delta\rho_{km}^{p} = b \cdot e^{p}. \tag{5}$$

The formation of double differences range is straightforward and given by

$$\nabla\Delta\rho_{km}^{pq} = b \cdot (e^{p} - e^{q}) = b \cdot e^{pq}. \tag{6}$$

The direction cosines are computed from the difference between the satellite and receiver positions. Note that, since the receiver-satellite distance is much bigger than the baseline length, it is assumed that a satellite's direction cosine is equal to both receivers.

Thus, the system that relates the baseline vector and the integer ambiguities with the observed double differences, for a constellation of n satellites is defined as

$$\begin{aligned}\begin{bmatrix}\nabla\Delta PR_{km}^{12}\\ \nabla\Delta PR_{km}^{13}\\ \vdots\\ \nabla\Delta PR_{km}^{1n}\\ \nabla\Delta\Phi_{km}^{12}\\ \nabla\Delta\Phi_{km}^{13}\\ \vdots\\ \nabla\Delta\Phi_{km}^{1n}\end{bmatrix} &= \begin{bmatrix}e_{km_x}^{12} & e_{km_y}^{12} & e_{km_z}^{12}\\ e_{km_x}^{13} & e_{km_y}^{13} & e_{km_z}^{13}\\ \vdots & \vdots & \vdots\\ e_{km_x}^{1n} & e_{km_y}^{1n} & e_{km_z}^{1n}\\ e_{km_x}^{12} & e_{km_y}^{12} & e_{km_z}^{12}\\ e_{km_x}^{13} & e_{km_y}^{13} & e_{km_z}^{13}\\ \vdots & \vdots & \vdots\\ e_{km_x}^{1n} & e_{km_y}^{1n} & e_{km_z}^{1n}\end{bmatrix}\begin{bmatrix}b_x\\ b_y\\ b_z\end{bmatrix} \dots \\ &+ \begin{bmatrix}0 & 0 & \cdots & 0\\ 0 & 0 & \cdots & 0\\ \vdots & \vdots & \ddots & \vdots\\ 0 & 0 & \dots & 0\\ \lambda & 0 & \dots & 0\\ 0 & \lambda & \dots & 0\\ \vdots & \vdots & \ddots & \vdots\\ 0 & 0 & 0 & \lambda\end{bmatrix}\begin{bmatrix}\nabla\Delta N_{km}^{12}\\ \nabla\Delta N_{km}^{13}\\ \vdots\\ \nabla\Delta N_{km}^{1n}\end{bmatrix} + \begin{bmatrix}\nabla\Delta\epsilon_{km}^{12}\\ \nabla\Delta\epsilon_{km}^{13}\\ \vdots\\ \nabla\Delta\epsilon_{km}^{1n}\\ \nabla\Delta\epsilon_{km}^{12}\\ \nabla\Delta\epsilon_{km}^{13}\\ \vdots\\ \nabla\Delta\epsilon_{km}^{1n}\end{bmatrix}.\end{aligned} \tag{7}$$

Note that the superscript 1 represents the reference satellite, selected as the one with highest elevation angle. This choice is done to optimize the geometry and reduce the system dilution of precision (DOP), [9].

The system defined above can be reduced to the form

$$y = Bb + Aa + e, \tag{8}$$

where,

- y is the observed vector of double differences ($\mathbb{R}^{2(n-1)\times 1}$);
- B is the system matrix for the baseline coordinates, containing the differenced direction cosines ($\mathbb{R}^{2(n-1)\times 3}$);
- b is the baseline coordinates' vector ($\mathbb{R}^{3\times 1}$);
- A is the system matrix for the integer ambiguity set ($\mathbb{R}^{2(n-1)\times(n-1)}$);
- a is the aforementioned integer ambiguity set ($\mathbb{R}^{(n-1)\times 1}$);
- e is the measurement noise vector, assumed to have Gaussian distribution, with expected value zero and covariance matrix Q_y, which is symmetric and positive defined, [4]. Since double differences are correlated, Q_y is not a diagonal matrix.

The system has solution if the constellation has, at least, four satellites, i.e. $n \geq 4$.

III. Baseline Determination and Integer Ambiguity Resolution

A. Float Solution

The solution for the system (8) can be determined resorting to a weighted least squares estimator, in order to minimize the error norm defined as, [6],

$$\|y - Bb - Aa\|_{Q_y^{-1}}^{2}, \tag{9}$$

where $\|e\|_{Q_y^{-1}}^{2} = e^{T}Q_y^{-1}e$. Thus, the estimator should be represented by

$$\begin{bmatrix}\hat{a}\\ \hat{b}\end{bmatrix} = \left([A \quad B]^T Q_y^{-1}[A \quad B]\right)^{-1}[A \quad B]^T Q_y^{-1} y. \tag{10}$$

Despite the error minimization, the estimator gives a floating point solution, which is not the correct value since the correct ambiguities are integers. In order to correctly determine the integer ambiguities, search techniques are used.

B. LAMBDA Method

The LAMBDA method (Least-Squares AMBiguity Decorrelation Adjustment) proposed in [4], is considered to be the most efficient search technique, accordingly to [6] and [13], So, it was used in this work and it will be presented in detail. It is composed by three steps: float solution, integer ambiguity estimation, and fixed solution, [5].

In the float solution step, the inaccurate solution obtained by the weighted least squares estimator, $\hat{a}$ in equation (10), is used in the search process as the central point. The error estimation covariance matrix, $Q_{\hat{a}}$, defines the search space to find the correct integer ambiguity vector, $\check{a}$, that minimizes the cost function $\|\hat{a} - a\|^2_{Q_{\hat{a}}}$,

$$\check{a} = arg\left(min_{a\in\mathbb{Z}} \|\hat{a} - a\|^2_{Q_{\hat{a}}}\right), \tag{11}$$

that is the integer ambiguity estimation step.

Due to the correlated nature of double differences (which leads to a non diagonal covariance matrix for double differences and, consequently, a non diagonal covariance matrix for the float solution) the search space is in general elliptical. The LAMBDA method uses a transformation matrix to decorrelate the error and, therefore, to diagonalize the covariance matrix of the float solution, creating a search space that is nearly spherical. This diagonalization is accomplished by a Z transformation defined as

$$Q_{\hat{z}} = Z^T Q_{\hat{a}} Z. \tag{12}$$

The next step is to decompose the covariance matrix of the float solution as

$$Q_{\hat{a}} = L^T D L, \tag{13}$$

where L is a lower matrix and D is a diagonal matrix. Knowing that the elements of Z are integers and that Z is close to L^{-1} one must have

$$Q_{\hat{z}} = \tilde{L}^T \tilde{D} \tilde{L}, \tag{14}$$

where the non diagonal elements of this new covariance matrix, represented by $\tilde{L}$, are close to zero, leading to a nearly diagonal covariance matrix. The matrix $\tilde{D}$ contains the diagonal elements.

After this decorrelation process, the new cost function is,

$$\check{z} = arg\left(min_z \|\hat{z} - z\|^2_{Q_{\hat{z}}}\right), \tag{15}$$

where $z = Z^T a$ and $\hat{z} = Z^T \hat{a}$, and hence the fixed solution is $\check{a} = Z^{-T}\check{z}$.

The volume of the search space is controlled by the value χ^2 that takes into account the new nearly diagonal covariance matrix and the number of candidates desired by the user. That is, the LAMBDA method outputs those ambiguities that verify the inequality

$$(\hat{z} - z)^T Q_{\hat{z}}^{-1} (\hat{z} - z) \leq \chi^2. \tag{16}$$

Note that the outputs are sorted in the ascending order of distance to the float solution.

C. Ambiguity Filter

Following the methodology developed in [9], the Ambiguity Filter developed in this paper chooses the best ambiguity set from the outputs from the LAMBDA method. For each candidate set $\check{a}$, as resulting from LAMBDA method, the correspondent baseline, $\check{b}(\check{a})$, is computed with the objective of assigning merit to each candidate.

The Ambiguity Filter is composed by three steps: validation, selection, and stabilization. Before the description of these three steps, the process of merit assignment will be described.

1) Merit Attribution

The merit attribution is done resorting to two tests. The first one, presented in [9], is the baseline length constraint. The second one, proposed in [14], makes use of the Up coordinate while the ambiguity set is not stabilized.

a) Baseline Length Constraint

With the knowledge of the real baseline distance, l, the error of the estimated baseline is obtained as

$$\delta_b = \left| \|\check{b}(\check{a})\| - l \right| \tag{17}$$

b) Up Coordinate Constraint

This test is similar to the previous one, but only considers the Up coordinate resulting from the candidate set that is being tested. It is assumed that during the initialization (i.e. while there is no stabilized solution) the platform is stopped, which leads to a constant baseline vector. By measuring the altitude difference between the reference antenna and the auxiliary one, it is possible to obtain the real Up coordinate, u_{real}. Thus, the Up coordinate error is given by

$$\delta_u = |\check{u}(\check{a}) - u_{real}|. \tag{18}$$

For each test defined above, the errors of the candidates are grouped in a vector with ascending order of the respective error, which is the descending order of merit. So, the merit, M, of a candidate set will be attributed according with position, i, of the error in the sorted vector, that is

$$M_i = 1/i. \tag{19}$$

2) Validation

The validation step makes use of the baseline length error, described by equation (17), and defining a threshold that was set to be $10\,cm$, due do the errors present in the baseline estimation. That is,

$$\delta_b = \left| \|\check{b}(\check{a})\| - l \right| \leq 0.1 \tag{20}$$

The candidates that have a baseline length error bigger than the threshold are excluded.

3) Selection

This step is where the merit is assigned. This is done by combining the two tests defined previously.

The candidate set with higher merit will be selected as the fixed solution for the respective epoch.

4) Stabilization

The candidate set selected as the fixed solution by the Ambiguity Filter in each epoch, is stored in a data base. As debated in [9], the ambiguity set that first achieves 50 occurrences as a fixed solution (i.e. a candidate is selected as the fixed solution in 50 different epochs) is the optimal fixed solution. Thereafter the optimal baseline vector will be determined by the optimal fixed solution.

In dynamic environments variations in the satellite constellation, like the change of the reference satellite, the loss of lock and cycle slips, occur quite often. To recover from these situations and avoid the resetting of the Ambiguity Filter, the solutions described in [9] and [14] are used.

IV. ATTITUDE DETERMINATION

A. Introduction

Using the Ambiguity Filter in the determination of multiple baselines it is possible to solve the attitude determination problem. In this paper three baselines (i.e. four GPS receivers) were used. Next, the technique used to determinate the Euler angles is descrived.

B. Quaternion-Based Extended Kalman Filter

1) Quaternion and Euler Angles

As an alternative to rotation matrices, a quaternion may be used as rotation operator, as described in [15]. A quaternion is a hyper-complex number of rank 4, and it is defined as

$$q = q_0 + iq_1 + jq_2 + kq_3,. \tag{21}$$

where q_0 is called the scalar part and $iq_1 + jq_2 + kq_3$ are called the vector part. An important property is that the quaternion q is unitary, that is,

$$\|q\|^2 = q_0^2 + q_1^2 + q_2^2 + q_3^2 = 1,. \tag{22}$$

which consists in a crucial constraint when using a quaternion for attitude determination, as presented in the development of the EKF, proposed in next section.

The attitude may be defined by the rotation transformation which relates a coordinate system fixed in space (North East Down – NED) to a coordinate system fixed in the body (XYZ: X – pointing in the moving direction; Z – point down; Y – orthogonal to the plane XZ). Due to its nature, the coordinates of the baselines will be constant in the XYZ frame. Thus, the matrix containing the baseline vectors (where each column is one vector) is given by

$$B_{NED} = A_q B_{xyz}. \tag{23}$$

where B_{xyz} is the matrix containing the baseline vectors in the body fixed frame and A_q is the rotation matrix in terms of the quaternion elements, that is

$$A_q = \cdots \begin{bmatrix} -1 + 2\binom{q_0^2 +}{q_1^2} & 2\binom{q_1 q_2 -}{q_0 q_3} & 2\binom{q_1 q_3 +}{q_0 q_2} \\ 2\binom{q_1 q_2 +}{q_0 q_3} & -1 + 2\binom{q_0^2 +}{q_2^2} & 2\binom{q_2 q_3 -}{q_0 q_1} \\ 2\binom{q_1 q_3 -}{q_0 q_2} & 2\binom{q_2 q_3 +}{q_0 q_1} & -1 + 2\binom{q_0^2 +}{q_3^2} \end{bmatrix}. \tag{24}$$

Finally, the Euler angles can be obtained from the quaternion matrix as

$$\begin{aligned} \theta &= sin^{-1}\left(-A_q^{31}\right), \\ \phi &= tan^{-1}\left(A_q^{32} \Big/ A_q^{33}\right), \\ \psi &= tan^{-1}\left(A_q^{21} \Big/ A_q^{11}\right), \end{aligned} \tag{25}$$

where the superscript in the matrix represents its index.

2) Extended Kalman Filter

To obtain the Euler angles based on the rotation quaternion it is necessary to estimate the parameters q_0, q_1, q_2 and q_3. The system dynamics of the quaternion is represented by

$$\dot{q} = \frac{1}{2}\Omega q, \tag{26}$$

where q is the vector containing the quaternion components, that is, $q = [q_0\ q_1\ q_2\ q_3]^T$, and Ω is the skew-symmetric matrix, defined as

$$\Omega = \begin{bmatrix} 0 & \omega_z & -\omega_y & \omega_x \\ -\omega_z & 0 & \omega_x & \omega_y \\ \omega_y & -\omega_x & 0 & \omega_z \\ -\omega_x & -\omega_y & -\omega_z & 0 \end{bmatrix}, \tag{27}$$

where $\omega = [\omega_x\ \omega_y\ \omega_z]^T$ are the angular velocities in the body frame axis. In this paper only GPS observables and its derivations are used as observations. Thus, the angular velocities must be estimated along with the quaternion components.

The continuous system (26) leads to a linear time-varying discrete system defined as

$$x_{k+1} = F(x_k)_k + G_k w_k, \tag{28}$$

with each component being

$$x_{k+1} = \begin{bmatrix} q_{k+1} \\ \omega_{k+1} \end{bmatrix}, \tag{29}$$

$$F_k = \begin{bmatrix} q_k + \frac{1}{2}\Delta t \Omega_k q_k \\ \omega_k \end{bmatrix}, \tag{30}$$

$$G_k = \begin{bmatrix} -\frac{1}{2}\Xi & 0 \\ 0 & I \end{bmatrix}, \tag{31}$$

$$\Xi = \begin{bmatrix} q_3 & -q_2 & q_1 \\ q_2 & q_3 & -q_0 \\ -q_1 & q_0 & q_3 \\ -q_0 & -q_1 & -q_2 \end{bmatrix}, \tag{32}$$

where Δt is the sampling ($\Delta t = 1\ s$ for the GPS case), w_k is the process noise, Gaussian distributed with zero mean and covariance Q, and $\Xi\omega = \Omega q$, accordingly to [16].

The measurement model relates the baselines' coordinates with the quaternion elements estimated by the EKF and the known positions of the GPS antennas in the body fixed frame, accordingly to (23). Additionally, the measurement model takes into account the unitary norm constraint of the quaternion, defined in (22). This is done by using this constraint has a perfect measurement, as described in [17]. Thus, the measurement model is non linear time-varying and has the form

$$z_k = h(x_k)_k + v_k, \tag{33}$$

where v_k is the measurement noise, Gaussian distributed with zero mean and covariance R, and

$$z_k = \begin{bmatrix} b_{NED}^{12} \\ b_{NED}^{13} \\ b_{NED}^{14} \\ 1 \end{bmatrix}, \tag{34}$$

$$h(x_k)_k = \begin{bmatrix} A_q b_{NED}^{12} \\ A_q b_{NED}^{13} \\ A_q b_{NED}^{14} \\ q^T q \end{bmatrix}. \tag{35}$$

Since the observation model is non linear, to estimate the quaternion components and the angular velocities it is necessary to implement an EKF, which in this case consists in the linearization of the measurement model around the nominal solution. This is done by Taylor Series expansions, where neglecting the high order terms (assumed to have small numeric values), [18], leads to the Jacobian matrices defined as

$$H_k = \begin{bmatrix} \frac{\partial h(x_k)_k}{\partial q} & \frac{\partial h(x_k)_k}{\partial \omega} \end{bmatrix}. \tag{36}$$

The process noise characterizes the small disturbance in the system's dynamics and is given by, [18] and [19],

$$Q_k = E[w_k w_k^T] = \cdots \int_{t_k}^{t_{k+1}} F(t_{k+1}, \tau) G(\tau) Q G^T(\tau) F^T(t_{k+1}, \tau)\, d\tau, \tag{37}$$

Where Q is a diagonal matrix containing the covariance of the disturbances present in the angular velocities, that is,

$$Q = \begin{bmatrix} Q_1 & 0 \\ 0 & Q_2 \end{bmatrix}_{6\times 6}, \tag{38}$$

where Q_1 is the covariance of the angular velocity noise and Q_2 is the covariance of the angular velocity bias noise, [16]. These two parameters must be tuned in order to obtain the best solution, but since it is not used any rate gyro, it is assumed that the value of Q_2 is close to zero. To solve (37) it is assumed that the time interval between two measurements is small enough to use the approximation

$$Q_k \approx G_k Q_k G_k^T \Delta t. \tag{39}$$

Since the measurements used are the coordinates of the baseline vectors (assumed to be independent), the measurement covariance matrix of each baseline is diagonal, with each component being the correspondent variance. Thus for the three baselines and the quaternion norm perfect measurement (noise free), the observation covariance matrix of the EKF is defined as

$$R_k = E[v_k v_k^T] = \cdots \begin{bmatrix} R_{NED}^{12} & 0 & 0 & 0 \\ 0 & R_{NED}^{13} & 0 & 0 \\ 0 & 0 & R_{NED}^{14} & 0 \\ 0 & 0 & 0 & 0 \end{bmatrix}, \tag{40}$$

where $R_{NED} = \begin{bmatrix} \sigma_N^2 & 0 & 0 \\ 0 & \sigma_E^2 & 0 \\ 0 & 0 & \sigma_D^2 \end{bmatrix}$ for the respective baseline.

Finally, the EKF has the form

$$\hat{x}_k^- = F_k x_k, \tag{41}$$

$$P_k^- = F_k P_{k-1} F_k^T + Q_k. \tag{42}$$

$$K_k = P_k^- H_k^T \left(H_k P_k^- H_k^T + R_k\right)^{-1}, \tag{43}$$

$$\hat{x}_k = \hat{x}_k^- + K_k(z_k - h(\hat{x}_k^-)_k), \tag{44}$$

$$P_k = (I - K_k H_k) P_k^-, \tag{45}$$

where the equations (41) and (42) consist in the prediction step. The remaining equations correspond to the update step, where the Kalman gain is determined and used to weight the state prediction based on the innovation process.

The developed EKF can provide a solution for the problem at hand and is unique.

V. RESULTS

The results presented in this section were made resorting to static and dynamic trials in urban scenarios (i.e. scenarios with multipath), and were obtained resorting to four Magellan AC12 GPS receivers, placed in the top of a car and at known positions in the body fixed frame. The placement of each GPS antenna is illustrated in Figure V.1, where the baselines' length are $\|b_{1-2}\| = \|b_{1-3}\| \approx 0{,}8\ m$ and $\|b_{1-4}\| \approx 1{,}35$. The term "Baseline 1-n" corresponds to the baseline vector between the receiver 1 and the receiver n.

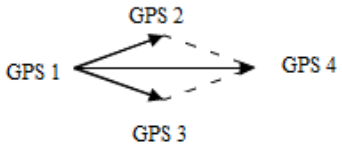

Figure V.1 – GPS receivers' disposition

Using the baseline vectors obtained with the Ambiguity Filter as measurements, after the algorithm's stabilization, the attitude angles were obtained by estimating the rotation quaternion resorting to the EKF.

A. Static Trials

The evolution of the attitude angles, computed with the estimated quaternion, is depicted in Figure V.1. Since the quaternion is estimated resorting to an EKF and this is a recursive algorithm, it takes a few seconds to stabilize in the correct values. In Figure V.3 is presented a zoom of the attitude angles' evolution, excluding the interval that corresponds to the estimation transitory.

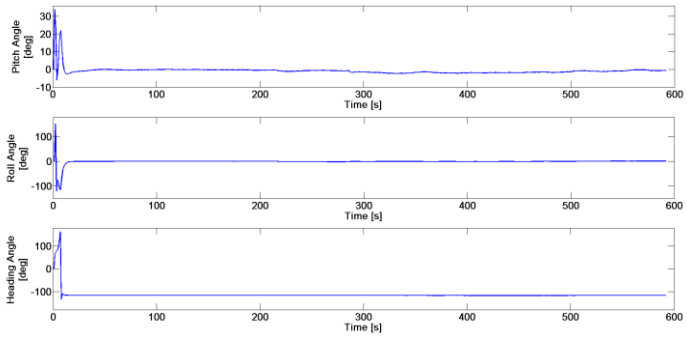

Figure V.2 – Evolution of the Euler angles for the static trial

The performance results presented in Table 1 show that the angles were obtained with precision levels smaller than 1° (1σ), which is good considering an urban environment.

As aforementioned, only the baseline vectors are used as measurements. Thus, the angular velocities are estimated in the EKF, and its evolution is depicted in Figure V.4. As expected, the presented results for the angular velocities converge to zero, since the platform has no motion.

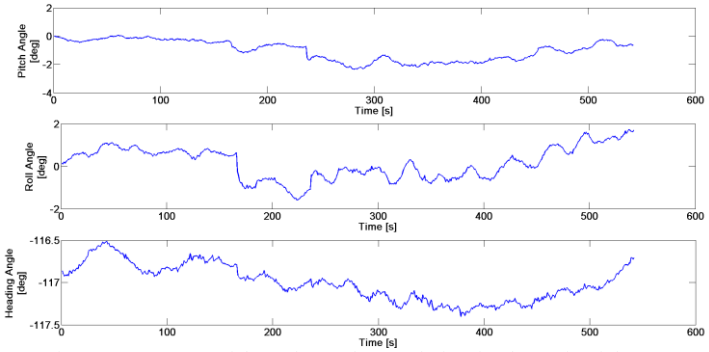

Figure V.3 – Zoom of the Euler angles' evolution for the static trial

Table 1 - Performance of the attitude angles estimation for the static trial

		Quaternion Based EKF
Pitch Angle	μ (°)	−1,007
	σ (°)	0,708
Roll Angle	μ (°)	0,147
	σ (°)	0,751
Heading Angle	μ (°)	−117,008
	σ (°)	0,212

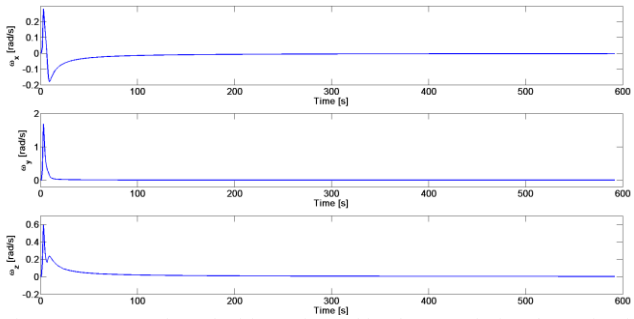

Figure V.4 – Angular velocities estimated by the EKF during the static trial

Since there is no information about the real value of the attitude angles, the innovation process may be used to evaluate the EKF performance. The innovation performance for each baseline is resumed in Table 2. The results show that the mean value of the innovation process is close to zero and that its precision is close to the millimeter-level.

Table 2 – Performance of the innovation process for each baseline, during the static trial

	Baseline 1-2	Baseline 1-3	Baseline 1-4
$\mu_{Innov.\ North}\ (m)$	0,020	0,011	0,004
$\sigma_{Innov.\ North}\ (m)$	0,003	0,006	0,008
$\mu_{Innov.\ East}\ (m)$	0,033	0,003	0,032
$\sigma_{Innov.\ East}\ (m)$	0,004	0,004	0,005
$\mu_{Innov.\ Down}\ (m)$	−0,009	−0,009	−0,017
$\sigma_{Innov.\ Down}\ (m)$	0,008	0,010	0,008

B. Dynamic Trials

The Euler angles' evolution, corresponding to the dynamic trial, is depicted in Figure V.5. Around the epoch $t = 150\ s$ the platform starts moving, which is characterized by the heading variation and the increase in the disturbances present in both pitch and roll angles. As for the static case, in the first epochs the EKF's solution is characterized by a transitory preceding the convergence of the state variables around the correct solution.

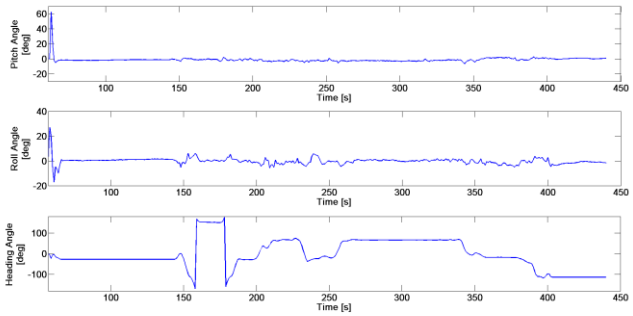

Figure V.5 – Evolution of the Euler angles for the dynamic trial

By analyzing the Figure V.5 along with the zoom of pitch and roll angles in Figure V.6, one may verify that at the beginning, around epoch $t = 150\ s$, of the trajectory the roll angle estimated by the EKF is highly disturbed when compared with the solution obtained by the rotation matrix. This fact is emphasized by the x term of the angular velocity after the platform start moving in Figure V.9, which is not exact since the maneuvers made during the trial were with small accelerations. This may be explained by the decrease of precision in the Up coordinate after the platform started moving, which is represented in Figure V.7. This could be improved by using an accelerometer output as measurement of the EKF and hence to better estimate the angular velocities.

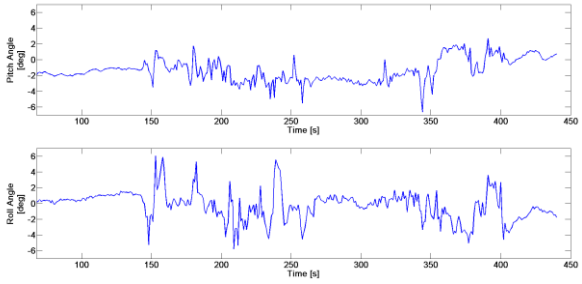

Figure V.6 – Zoom of pitch and roll angles for the dynamic trial

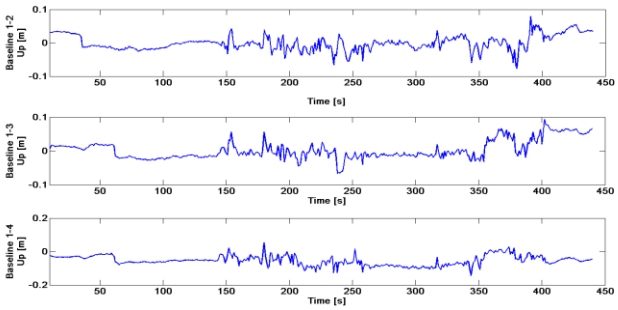

Figure V.7 – Up coordinate evolution of the three baselines after stabilization

During this trial a positive roll angle was imposed to the car used as platform by climbing the side walk only with the left side wheels, between epochs $t \in [235; 245]\ s$ and when the vehicle's heading was $\approx -30°$. This test's result is depicted in Figure V.8, where it is possible to see that the roll angle evolution is approximately 5° at epoch $t = 240\ s$, which corresponds to the positive rotation about the x-axis applied to the vehicle.

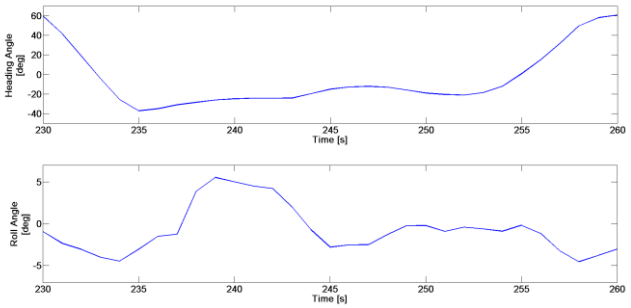

Figure V.8 – Zoom of heading and roll angles, during a positive rotation about the $\boldsymbol{x}$ axis (positive roll angle), for the dynamic trial

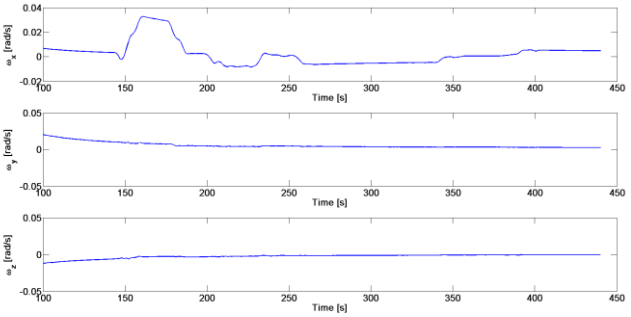

Figure V.9 – Evolution of the angular velocities estimated by the EKF during the dynamic trial

In the dynamic trial case, the movement increased the disturbances present in the measurements as already illustrated in Figure V.7 for the baselines' Up coordinates. This fact is illustrated too in the performance of the EKF, which is resumed in Table 3, where it is possible to confirm that the average innovation for each baseline is around zero and that the standard deviation varies from several millimeters to several centimeters, representing a slight degradation as expected when comparing with the results for the static trial in Table 2.

Table 3 – Performance of the innovation process for each baseline, during the dynamic trial

	Baseline 1-2	**Baseline 1-3**	**Baseline 1-4**
$\mu_{Innov.\ North}\ (m)$	−0,015	−0,007	−0,021
$\sigma_{Innov.\ North}\ (m)$	0,066	0,070	0,107
$\mu_{Innov.\ East}\ (m)$	0,007	0,002	−0,006
$\sigma_{Innov.\ East}\ (m)$	0,076	0,069	0,125
$\mu_{Innov.\ Down}\ (m)$	−0,011	−0,011	0,015
$\sigma_{Innov.\ Down}\ (m)$	0,027	0,024	0,033

Despite the degradation of the disturbances in a dynamic trial, the EKF performance is good and the results validate this technique.

VI. CONCLUSIONS

The static trial results showed that the quaternion based EKF based on multiple baselines estimate the Euler angles with precisions smaller than 1° (1σ).

Despite the disturbances augmentation, the dynamic results are representative of the successfully implementation of the attitude determination algorithm, capable of detecting attitude variations along the path made by the test platform, as

depicted for the positive roll test. The increase in the level of disturbances is visible in the attitude angles that are function of the Up coordinate (which is more sensible to noise), that is, pitch and roll angles. The roll angle is more affected by this phenomenon, since the highly disturbed Up coordinate led to a highly disturbed angular velocity about the x axis. However these disturbances do not affect the correct determination of the Euler angles, which is proved by the performance of the EKF innovation. This could be improved by using an INS sensor, in order to better estimate the angular velocities. Despite the disturbances' augmentation, the innovation has errors in the order of the centimeter (1σ).

ACKNOWLEDGMENT

This work was partially supported by the Instituto de Telecomunicações (IT), the Institute for Systems and Robotics ISR) and the Portuguese Foundation for the Science and Technology (FCT) – Project PTDC/EEA-TEL/122086/2010.

REFERENCES

[1] B. L. V. Kuylen, P. Nemry, F. Boon, A. Simsky, and S. Nv, "Comparison of Attitude Performance for Multi-Antenna Receivers," *European Journal of Navigation*, vol. 4, nº2, pp. 1-9, May 2006.

[2] E. D. Kaplan and C. J. Hegarty, *Understanding GPS: principles and applications*, 2nd ed. Artech House Publishers, 2006.

[3] P. Misra and P. Enge, *Global Positioning System : Signals , Measurements , and Performance*, 2nd ed. Ganga-Jamuna Press, 2006.

[4] P. Teunissen, "Least-Squares Estimation of the Integer GPS Ambiguities," *Delft Geodetic Computing Centre LGR series*, No. 6, 16pp.

[5] P. J. D. Jonge, C. C. J. M. Tiberius, and P. J. G. Teunissen, "Computational Aspects of the LAMBDA Method for GPS Ambiguity Resolution," *Proceedings of ION GPS-96, 9th International Technical Meeting of the Satellite Division of the Institute of Navigation, Kansas City, Missouri*, Sept. 17-20, pp 935-944.

[6] G. Strang and K. Borre, *Linear algebra, geodesy, and GPS*. Wellesley Cambridge Pr, 1997.

[7] P. Teunissen, "The LAMBDA Method for the GNSS Compass," *Artificial Satellites-Journal of Planetary Geodesy,* Vol. 41, nº 3, pp 89-103, 2006.

[8] G. Giorgi and P. J. G. Teunissen, "Carrier Phase GNSS Attitude Determination with the Multivariate Constrained LAMBDA Method," *IEEE Aerospace Conference, Big Sky, MT*, pp. 1-12, Mar. 2010.

[9] J. Reis, "Real-time GPS Heading Determination," MSc Thesis, Instituto Superior Técnico, Technical University of Lisbon, November 2009.

[10] J. Reis, J. Sanguino, and A. Rodrigues, "Baseline Influence on Single-Frequency GPS Precise Heading Estimation," in *Wireless Personal Communications Journal*, Springer Netherlands, 2012.

[11] J. Reis, J. Sanguino, and A. Rodrigues, "Impact of Satellite Coverage in Single-Frequency Precise Heading Determination," in *Position Location and Navigation Symposium (PLANS), IEEE/ION*, 2010, Indian Wells, USA, 3-6 May 2010, pp. 592-597.

[12] J. Reis, J. Sanguino, and A. Rodrigues, "Influence of Baseline Length in Single-Frequency Real-Time Vehicle Heading Estimation," in *The 13th International Symposium on Wireless Personal Multimedia Communications (WPMC)*, Recife, Brazil, 11-14 October 2010.

[13] D. Kim and R. B. Langley, "GPS Ambiguity Resolution and Validation : Methodologies , Trends and Issues," *in International Symposium on GPS/GNSS*, Seoul, Korea, 2000.

[14] J. Cóias, J. Sanguino and P. Oliveira, "Attitude Determination Using the Ambiguity Filter with Single-Frequency L1 GPS Receivers," *in International Conference on Localization and GNSS*, Starnberg, Germany, June, 2012 (accepted for presentation).

[15] J. B. Kuipers, *Quaternions and rotation sequences*, vol. 1. Princeton university press Princeton, NJ, 1999.

[16] Y. T. Chiang, L. S. Wang, F. R. Chang, and H. M. Peng, "Constrained Filtering Method for Attitude Determination using GPS and Gyro," *IEE Proceedings - Radar, Sonar and Navigation*, vol. 149, no. 5, p. 258, 2002.

[17] D. Simon, *Optimal state estimation: Kalman, H [infinity] and nonlinear approaches*. John Wiley and Sons, 2006.

[18] Y. Bar-Shalom, X. Li, and T. Kirubarajan, *Estimation with applications to tracking and navigation*, vol. 9. 2001.

[19] F. Nunes, Lecture Notes on: "Sistemas de Controlo de Tráfego," 2010